Available online at www.sciencedirect.com

ScienceDirect

materialstoday: PROCEEDINGS

[Materials Today: Nanotexnology 2020 Proceedings]

A Mathematical Model of COVID-19 Transmission

Y. Tang[a], R. Jayatilaka[a], R. Patel[a], M. Brar[a], N. M. Jisrawi[a,b], S. R. Valluri[a,b1]

[a]*Department of Physics and Astronomy, Western University, 1151 Richmond Street, London N6A 3K7, Canada*
[b]*King's University College, Western University, 266 Epworth Avenue, London N6A 2M3, Canada*

Abstract

Disease transmission is studied through disciplines like epidemiology, applied mathematics, and statistics. Mathematical simulation models for transmission have implications in solving public and personal health challenges. The SIR model uses a compartmental approach including dynamic and nonlinear behavior of transmission through three factors: susceptible, infected, and removed (recovered and deceased) individuals. Using the Lambert W Function, we propose a framework to study solutions of the SIR model. This demonstrates the applications of COVID-19 transmission data to model the spread of a real-world disease. Physical distancing impacts and personal protection equipment use will be discussed in relevance to the COVID-19 spread.

Keywords: Lambert W function; SIR model; SEIR model; Nonlinear differential equations; Disease transmission.

1. Introduction

The First World War ravaged the world with death and destruction. A key contributor to the enormous death toll was not a factor of the war, but a product of its chaotic environment; the 1918 "Spanish" Influenza. This H1N1 virus of avian origin spread throughout 1918-1919, infecting over 500 million individuals (a third of the total world population at the time), and killing at least 40 million people worldwide [37, 21]. The lack of sanitation and resources during wartime, and no progress in the development of a vaccine limited worldwide control efforts to non-pharmaceutical interventions such as isolation, quarantine and use of informal disinfectants [14]. These procedures, however, were unevenly administered throughout the world, affecting spread of disease, and hindering the ability of countries to take care of their citizens [14]. Due to the immense, rapid spread of disease, countries were unable to suitably prepare themselves to prevent or control the influenza.

Now, almost a century later, the world is rocked again by the emergence of the new strand of coronavirus disease (COVID-19). This novel virus was first reported in December 2019 in Wuhan, China and has since spread throughout the world causing a global pandemic [31]. This virus can be transmitted person to person, causing great public concern [31]. Many measures have been put in place to keep human interactions to a minimum such as wearing a mask in public, keeping a two-metre distance between individuals and sanitization.

COVID-19 targets the human respiratory system, resulting in clinical findings such as high fever, dyspnea and invasive multilobed lesions as seen in chest radiographs [30, 19]. It has been reported that the symptoms of this virus start about 5 days after contracting it [31]. These symptoms tend to get progressively worse as time goes on, some cases leading to death, while others successfully recover [19]. This is a major public threat since thousands of Canadians have been hospitalized due to respiratory issues along with other flu like symptoms after being diagnosed with COVID-19 with no concrete vaccine yet developed [31].

1Corresponding author. Tel.: 519 661 2111 (ext. 86499); fax: 519 661 2033.
E-mail address: valluri@uwo.ca

While the world now has the advantage of more accessible resources and a better understanding of pandemics compared to 1918, there are still the problems of disease prevention and control. A way to combat this is to model the disease over time, to better understand the gravity of the situation [6]. Using data of epidemic curves, one can extrapolate disease data and trends to prepare for potential disease burden and determine public policies in order to mitigate risks of spread [6].

Epidemics play a major role in understanding disease transmission by studying disease distribution, sources of diseases, causes of diseases, and methods of disease control [17]. All these branches are important topics when making vaccines for diseases and for studying the transmission of diseases worldwide. The Susceptible-Infected-Removed (SIR) model and its derivatives is one way to understand the transmission of diseases and predict future outcomes regarding COVID-19 cases. This study uses the Lambert W function in the SIR model, SIRm model, Susceptible-Exposed-Infected-Removed (SEIR) model, and the SEIRm to illustrate the pandemic of COVID-19.

Section 2 of this paper discusses the data and methods that were used to illustrate COVID-19 trends through different models such as the SIR, SIRm, SEIR and the SEIRm models. By using Canadian data to model the current trend of COVID-19, it is possible to create a graph that can depict where the individuals stand in-time with the longevity of the disease. Using a mixing factor *m*, it is possible to introduce a human-behaviour or social distancing factor into the equation as shown in the SIRm and SEIRm models. Section 3 will present the results of our paper with multiple graphs to represent various mathematical models; there will be simulations of Canadian COVID-19 data in context of the afore-mentioned models. In Section 4, the results obtained from our analysis – particularly the plots in context of the SEIR model - will be discussed. Finally, Section 5 of this paper presents our conclusions.

2. Methods

In this study, open-source COVID-19 datasets provided by Public Health Agency of Canada's Public Health Infobase is used. The data ranges from January 1, 2020 to September 9, 2020, with each time series tracking an epidemiology statistic. The three-time series of focus are count of confirmed cases, deaths, and recovered cases nation-wide in Canada.

2.1. SIR Model

The SIR model is a representation that divides a population with respect to a disease's impact on an individual over time. An individual can be categorized as susceptible ($S(t)$), infected ($I(t)$) or removed ($R(t)$, dead or cured), denoted by S, I and R respectively, along an independent variable; time [33]. One of the most common SIR models is the classic Kermack–McKendrick Model for contagious diseases in a closed population over time. The model was created to illustrate the rapid changes in number of infected patients during epidemics. It is assumed that there is a fixed homogeneous population size, instantaneous incubation period, and acute onset of disease [15, 32, 16]. The model variables can be represented as fractions;

$$s = \frac{S}{N} \tag{1}$$

where s is a fractional representation of the number of susceptible individuals (S) over a selected population (N) over time.

$$i = \frac{I}{N} \tag{2}$$

where i is a fractional representation of the number of infected individuals (I) over a selected population (N) over time.

$$r = \frac{R}{N} \tag{3}$$

and r is a fractional representation of the number of removed individuals (R) over a selected population (N) over time.

Overall, these equations must add to 1:

$$s + i + r = 1 \tag{4}$$

Using these equations, it is possible to extract three nonlinear differential equations that can aid in tracking the progress of an illness. We present these equations below.

The Susceptible Equation:

$$\frac{ds}{dt} = -\beta si \tag{5}$$

where β represents the infection rate which is the probability per day that an I-person can infect a S-person. This includes daily mundane activities such as going to work or school, large gatherings, etc., assuming the absence of social distancing. The SIR model assumes that the population is randomly mixed.

The Infected Equation:

$$\frac{di}{dt} = \beta si - \gamma i \tag{6}$$

The Recovered Equation:

$$\frac{dr}{dt} = \gamma i \tag{7}$$

where γ represents the recovery rate which is the probability per day that an I-person transitions into an R-person; becoming non-infectious permanently.

The ratio of S-persons transitioning into I-persons is the ratio of β to γ, referred to as the Reproduction Number; λ.

$$\lambda = \frac{\beta}{\gamma} \tag{8}$$

The higher the value of λ, the more transmittable the disease is; this is as the infection rate eclipses the recovery rate.

While R_0 usually denotes the reproduction number, in this paper the symbol R_0 is used to denote the initial value of the Recovered variable at time $t = t_0$.

There is always some natural immunity, so it is reasonable to assume that r_0 is greater than 0. If the population has been partly vaccinated, the value of r_0 might even be 0.40 or more. Similarly, even without vaccination, a prior asymptomatic spread of the disease in the population may have resulted in r_0 being perhaps 15 or 20 percent of the population [1].

Some other variables can be introduced for the SIR model, for convenience of comparison with information reported about the course of the epidemic. The total number of cases since the beginning of the epidemic is C. The initial value of the total number of cases, prior to time $t = t_0$, is C_0. The number of new cases per day is J. The variable J is defined by

$$J = \frac{dC}{dt} = \beta \frac{SI}{N} \tag{9a}$$

Therefore, considering a closed population ($N = 1$) this equation becomes:

$$j = \beta si \tag{9b}$$

where j is the number of cases per day in a closed population.

There is a possibility that some individuals may have been included in the R-group due to natural immunity or vaccination immunity, rather than as recovered cases. Therefore, by tracking the decline in S-persons, it is possible to track the increase in total cases, c, while excluding the individuals with immunity [1]. This indicates

that *s* can be used as an independent variable to find *i* as a function of *s*;

$$i(s) = 1 - s - r(s) \tag{10a}$$

where *r*(*s*) can be written as $r_0 - \frac{1}{\lambda}\ln\left(\frac{s}{s_0}\right)$

$$i(s) = 1 - s - r_0 + \frac{1}{\lambda} ln\left(\frac{s}{s_0}\right) \tag{10b}$$

Dividing equation 6 by equation 5 results in:

$$\frac{di}{ds} = \frac{\gamma - \beta s}{\beta s} \tag{11}$$

The solution of this equation gives a Lambert W Function as implicitly seen in the expression given in equation (10b). This remarkable function has created a renaissance in the solution of diverse problems in innumerable fields of knowledge [9].

To continue, it is possible to use *r* as an independent variable as well. The expressions of *s* can be found with respect to *r*;

$$s(r) = s_0 exp[-\lambda(r - r_0)] \tag{12a}$$

which can then be substituted into the equation:

$$\frac{di}{dr} = \frac{\beta s - \gamma}{\gamma} = \lambda s - 1 \tag{12b}$$

to give:

$$\frac{di}{dr} = \lambda s_0 exp[-\lambda(r - r_0)] - 1 \tag{12c}$$

This equation (12c) can be integrated to provide an equation that illustrates *i* as a function of *r*:

$$i(r) = i_0 + s_0\{1 - exp[-\lambda(r - r_0)]\} - (r - r_0) \tag{13a}$$

$$i(r) = 1 - r - s_0 exp[-\lambda(r - r_0)] \tag{13b}$$

If there are very few infectious people, the I-group becomes a very small fraction of the population, therefore $s + r \approx 1$. In addition, peak infections occur when $\frac{di}{dt} = 0$, the time when the I-group is the largest, assuming $t = t_1$ at I_{max}, it is possible to rework the Infection Equation as;

$$\beta s(t_1) i(t_1) = \gamma(t_1) i(t_1) \tag{14a}$$

$$\beta s(t_1) = \gamma \tag{14b}$$

$$s(t_1) = \frac{\gamma}{\beta} = \frac{1}{\lambda} \tag{14c}$$

Therefore, the lower the value of λ, the larger the number of people entering the R-group. This is as the recovery rate will overpower the rate of individuals entering the I-group.

When $\lambda < 1$; $\gamma > \beta$. This indicates that the *s(t)* curve will decrease past *r(t)* curve, which will increase. When $\lambda = 1$, the ratios of *s(t)* and *r(t)* are equal and will inverse after the point of equivalence. When $\lambda < 1$, the ratio of

s(t) was greater than *r(t)*. This demonstrates that the *i(t)* value was increasing as the infection rate, β, is greater than the recovery rate, γ. A point of inflection occurs in the *i(t)* curve at $I_{max} = t_1$ which illustrates that as the ratios inverse between the *s(t)* and *r(t)* curves. The λ value decreases, indicating a lower β value; implying a decrease in members in the I-group and a descending *i(t)* curve.

The value of the inflection points can be found using the second derivative of *s* with respects to *t*;

$$\frac{d^2s}{dt^2} = -\beta \frac{d}{dt}[si] \tag{15}$$

As the epidemic dies out, the number of infectious people approaches zero, so an asymptotic limit is formed; $t \to \infty$, and therefore, $s + r = 1$.

2.1.1 SIRm Model

The SIRm model, as derived from the SIR model, places focus on the relationship between disease transmission and the effect of public health measures. Consider a situation in which public health guidelines are introduced to slow the frequency, duration and closeness of contact between S-people and I-people. This can be represented by making the value of the parameter β vary with time. However, a conceptually simpler way to describe such public health measures is to keep β constant and multiply it by a time-varying mixing factor *m* to reflect changes in social distancing. In the present section, we assume that β is constant, and develop the equations and approximations for the standard SIR model by setting all *m* values to 1.

As such, the differential equations in population fraction notation are:

$$\frac{ds}{dt} = -\beta msi \tag{16}$$

$$\frac{di}{dt} = \beta msi - \gamma i \tag{17}$$

$$\frac{dr}{dt} = \gamma i \tag{18}$$

$$s + i + r = 1 \tag{19}$$

Dividing equation (17) by equation (16) results in:

$$\frac{di}{ds} = \frac{-\beta ms + \gamma}{\beta ms} \tag{20a}$$

The solution of equation of (20a) is given as:

$$\frac{-\beta ms}{\gamma} = W\left(\frac{-\beta m}{\gamma}\right)^{\frac{-\beta m}{\gamma}} \tag{20b}$$

This equation is in terms of the Lambert W function, which is defined after equation (27) below.

The equations for total cases per day, *j*, and the total cumulative cases, *c* are [29]:

$$j = \frac{dc}{dt} \tag{21a}$$

or

$$j = \beta msi \tag{21b}$$

and

$$c = c_0 + \int_0^t j(\tau)\, d\tau \tag{22a}$$

or

$$c = c_0 + \beta \int_0^t m(\tau)s(\tau)i(\tau)\, d\tau \tag{22b}$$

2.2. SEIR Model

The SIR model can be extended using the Susceptible-Exposed-Infected-Removed (SEIR) variant. This model is like the SIR in that it also considers the susceptible, infected and removed populations but differs in that it also considers the exposed population; those who are incubating the virus but not infectious [22]. The SEIR model adds another layer of complexity to the SIR model, by allowing the analysis of conditions of susceptible and infected populations during an epidemic outbreak [12].

The SEIR model's governing equations are:

$$\frac{dS}{dt} = -\rho\beta si \tag{23}$$

$$\frac{dE}{dt} = \rho\beta si - \alpha e \tag{24}$$

$$\frac{dI}{dt} = \alpha e - \gamma i \tag{25}$$

$$\frac{dR}{dt} = \gamma i \tag{26}$$

where the parameters are defined as:
α: incubation rate from the exposed group to the infected group
β: infection rate
γ: removal rate from the infected group to removed group
ρ: the reduced spread rate factor ($0 \leq \rho < 1$)

The above parameters and equations compose the SEIR model [5, 28]. The equations have been modified to properly reflect a closed population.

This study examines the use of the Lambert W function in conjunction with the SIR and SEIR models, the multivalued inverse of the function $w \rightarrow we^w$ [9]. In the 18th century, scientist Johann Lambert gave a solution to a trinomial equation, upon which further work by Euler and Sir Edward Wright led to the now modern definition of Lambert's original work [39]. Their function, named to honour Lambert, is as follows:

$$W(z)e^{W(z)} = z \tag{27}$$

The Lambert W function is implicitly elementary in that it is defined by an equation composed of only elementary functions, but is not an elementary function itself. It has applications in a variety of fields ranging from

quantum physics, black holes to even the spread of disease [13].

Corless et al.'s article regarding the Lambert W function further studied the function's applicability in epidemics. In terms of epidemics and components, let us assume in a population of *n* people, everyone has same contact with α random others [9]. If γ is the weak connectivity of this random net, and disease spreads through transitivity to those in close contact with the infected individual, the total infected population is approximated as γn for large n, where:

$$\gamma = 1 - e^{-\alpha \cdot \gamma} \tag{28}$$

This formula can also be applied for conditions where α is a fixed integer, as well as when α is an expected value in that it not fixed for all individuals and may not be an integer [34, 18]. Re-writing the above formula are:

$$\alpha e^{\alpha} = \alpha(1-\gamma)e^{\alpha(\gamma-1)} \tag{29a}$$

One can determine:

$$\gamma = 1 - T\frac{(\alpha e^{-\alpha})}{\alpha} = 1 + W\frac{(\alpha e^{-\alpha})}{\alpha} \tag{29b}$$

where $\alpha \geq 1$, using the principal branch of T (of the Tree function) and W (of the Lambert W function) [9].

This epidemic problem is closely tied to a phenomenon described by Erdös and Rényi in which the epidemic problem is related to the size of the 'giant component' in a random graph [11]. Essentially, when a graph on *n* vertices with $m = \frac{1}{2}\alpha n$ edges is randomly chosen, it is almost certain it has a connected component with approximately γn vertices (for γ given by equation (2)) when $\alpha \geq 1$ [9].

2.2.1. *SEIRm Model*

The SEIRm model is a derivation of the SEIR model that was discussed above. The SEIRm model trials demonstrate various stabilities of the COVID-19 virus situation, based on unpublished report and private communications by Dr. Ken Roberts [38]. By observing the value of *m*, the severity of the situation can be determined. A higher *m* value would mean that there is high infectivity which not only effects the volume of patients in the hospital, but various other aspects related to COVID-19 [38]. If the *m* value is lower, then that would demonstrate a more manageable and in control situation [38]. This once again puts an emphasis on the importance of social distancing in order to maintain a lower *m* value. Hospitals would not have a mass increase in patient volume and the development of various medical equipment, and a vaccine can stay on track. Two very important aspects that would be affected by the reported COVID-19 cases are the development of a vaccine for COVID-19 and medical equipment for patients and for hospital staff. In SEIRm model trials. COVID-19 data for Ontario is used and $\alpha = 0.20$ and $\gamma = 0.20$, which gives $\beta = 0.81$ and $\lambda \approx 4$ [38].

2.3. *Planck Blackbody Distribution*

While analyzing several SIR models of disease, it was observed that some of the infection curves looked like Planck's blackbody distribution curves due to the realistic asymmetry of the infection data curves [24]. Keeping this in perspective, it was decided this study would simulate infection curves using an asymmetric function rather than a purely symmetric one. Max Planck theorized that mode energies of the blackbody are not continuously distributed but are quantized. He devised a law for blackbody radiation as follows [3]:

$$B_v(T) = A\frac{\left(2 \cdot h \cdot \nu^{\alpha}/_{c^2}\right)}{e^{h \cdot \nu/_{kT}-1}},\ \alpha{=}3 \tag{30}$$

where B_v represents the spectral radiance**,** *h* represents the Planck constant; *c* represents the speed of light in a vacuum; *k* represents the Boltzmann constant; and *v* represents the frequency of the electromagnetic radiation; *T* represents the absolute temperature of the body; and α can take any value other than 3 to run Planck-like simulations in other situations. Therefore, this formula represents the spectral-energy distribution

of radiation emitted by a blackbody.

The similarity of the SIR model infection curve suggests that it may be reasonable to model the infection curve for a few different values of α like in a Planck Blackbody Distribution function with an appropriate definition of the constants C_1 and C_2 [39].

In this paper, two adjusted formulas inspired from the Planck Blackbody Distribution are proposed to model infection as a function of time.

$$I(t) = \frac{(C_2 \cdot t^{\alpha})}{e^{C_1 \cdot t} - 1} \tag{31}$$

where α can be 2 or 3, as represented in this study.

3. Results

3.1. *SIR Model*

Figures 1, 2, and 3 display the results of the SIR models fitted onto the given Canadian COVID-19 dataset by optimizing the MSE (mean square error) through the L-BFGS-B (Limited-memory Broyden-Fletcher-Goldfarb-Shanno with Boundaries) algorithm.

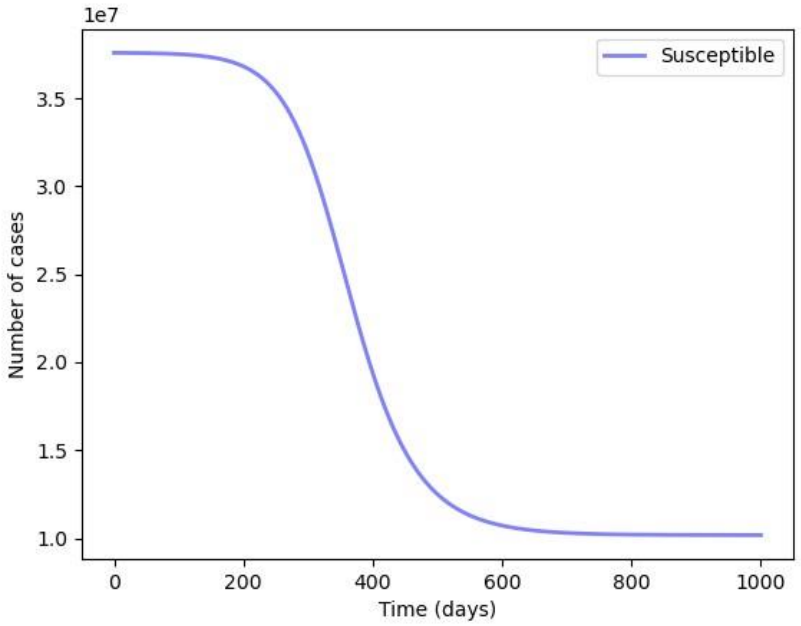

Fig.1. SIR Model's Susceptible Curve

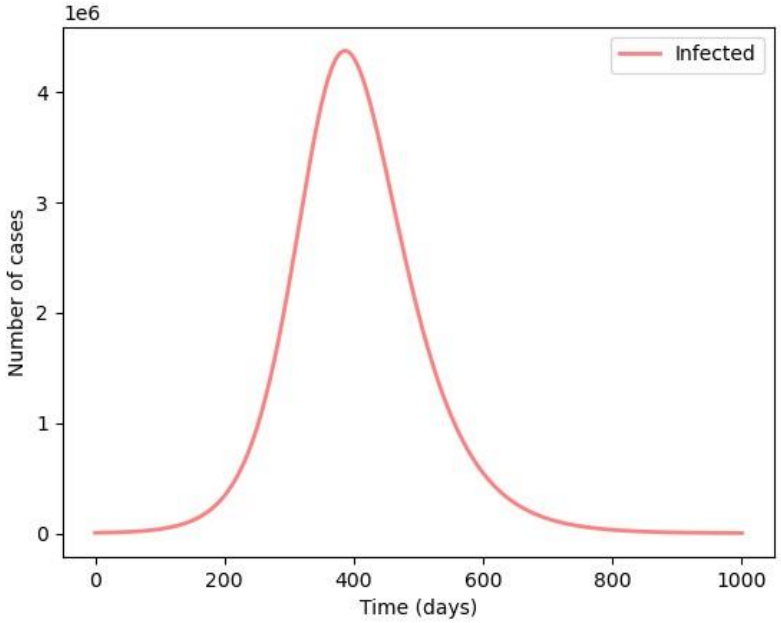

Fig. 2. SIR Model's Infected Curve

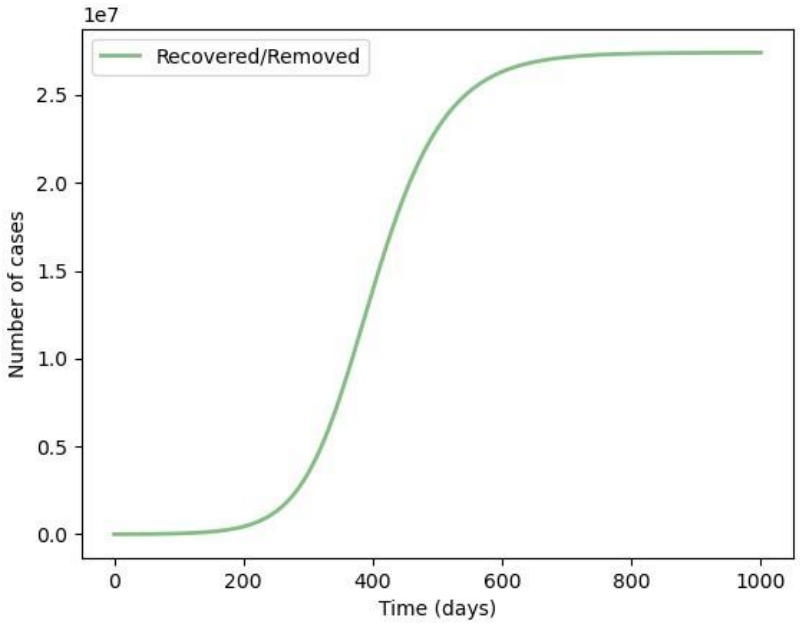

Fig. 3. SIR Model's Removed Curve

The SIR model parameters were derived through least-squared optimization. β is estimated to be 0.05076, and γ is estimated to be 0.028328. The figures suggest a continuation in the decreasing trend for susceptible and increasing trend for infected and recovered/removed.

3.2. *SEIR Model*

Figures 4, 5, 6, and 7 display the results of the adjusted SEIR models fitted onto the given Canadian COVID-19 dataset by optimizing the MSE through the L-BFGS-B algorithm.

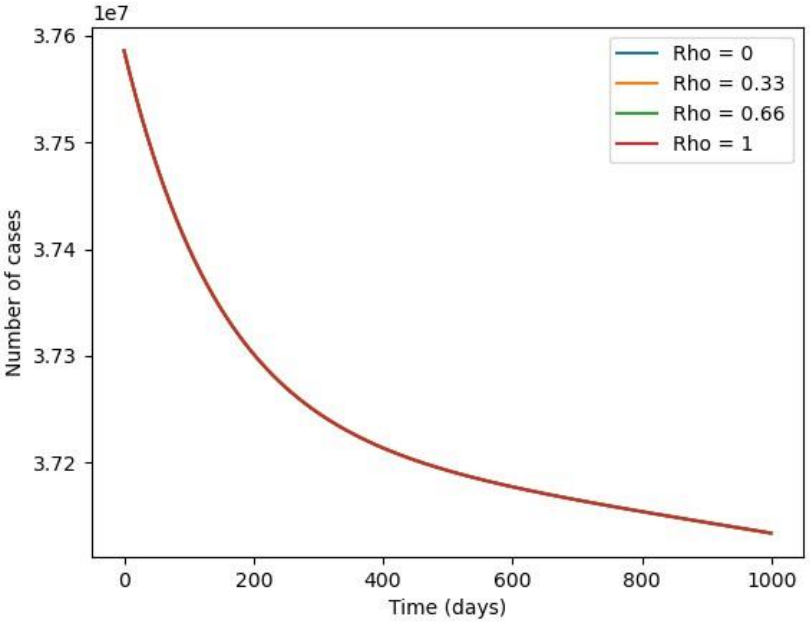

Fig.4. Effects of Social Distancing on SEIR Model's Susceptible Curve

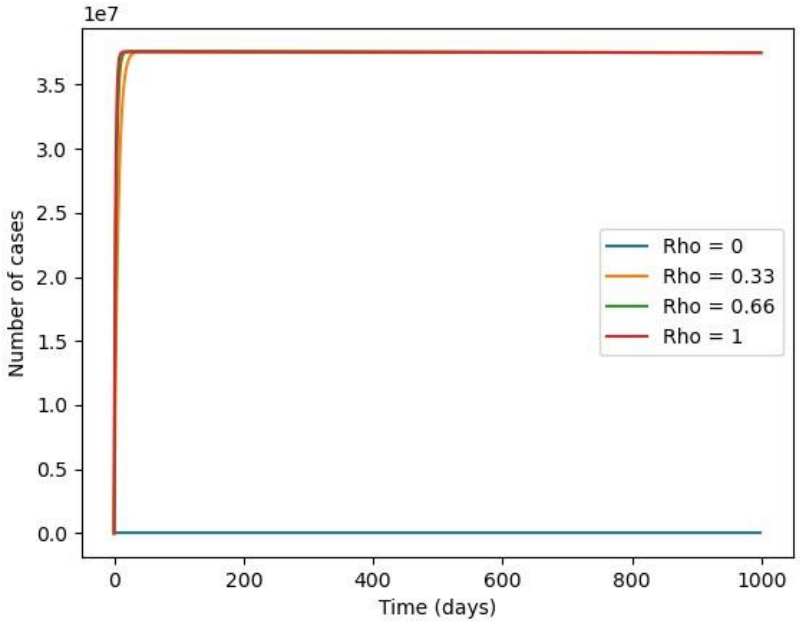

Fig.5. Effects of Social Distancing on SEIR Model's Exposed Curve

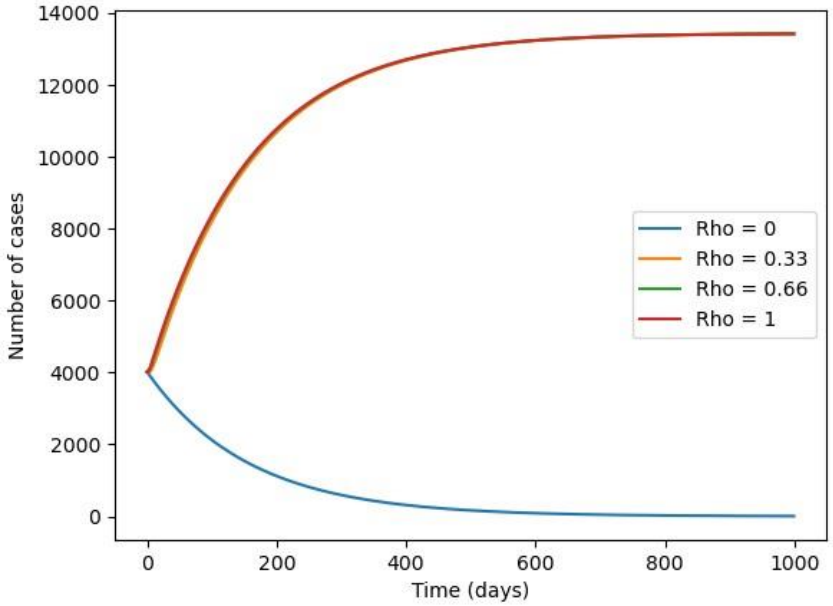

Fig.6. Effects of Social Distancing on SEIR Model's Infected Curve

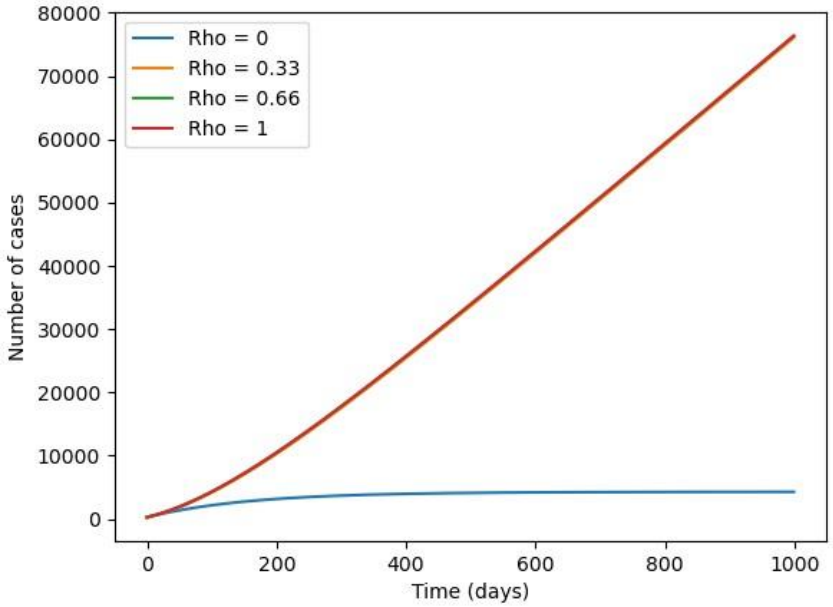

Fig.7. Effects of Social Distancing on SEIR Model's Removed Curve

The SEIR model parameters were derived through least-squared optimization. The population (N) considered was 3759000. α, β, γ, and ρ are estimated to be 2.142744e-05, 0.000130, 0.007435, and 0.000130 respectively.

In order to demonstrate the effect of social distancing, different measures of ρ were used to compare the difference in results. The figures suggest social distancing indeed provides positive value in terms of the containment of COVID-19. Note that $\rho = 0$ implies everyone in the society is quarantined, while $\rho = 1$ implies

no social distancing.

3.3. *Planck Blackbody Function*

Figures 8 and 9 display the results of the predicted infected curves after fitting the adjusted Planck Blackbody Distribution to the given Canadian COVID-19 dataset by optimizing the MSE through the Nelder-Mead algorithm. The parameters C_1 and C_2 were arrived through least-squared optimization.

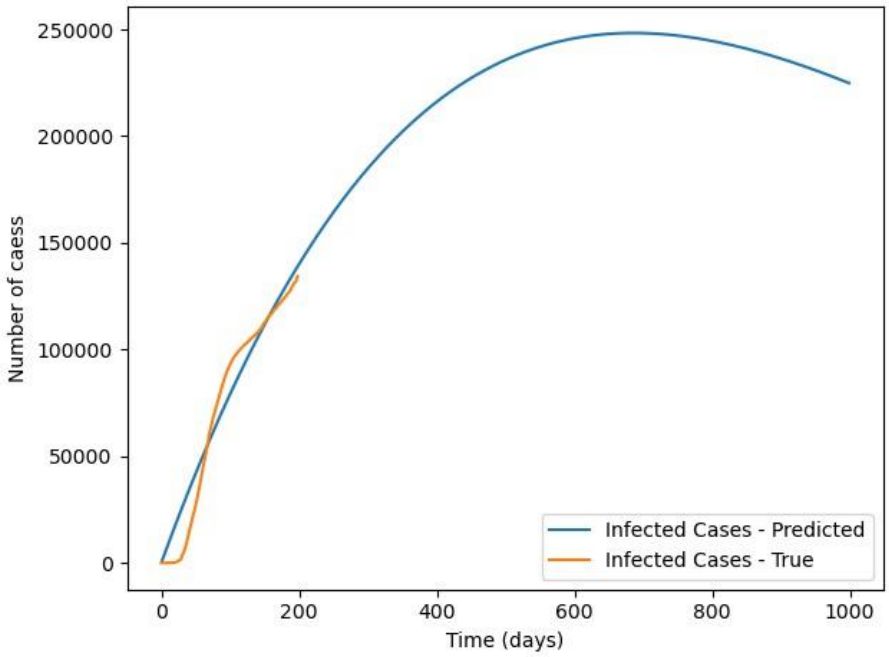

Fig.8. Infection Modelling using a Planck Function (α=2)

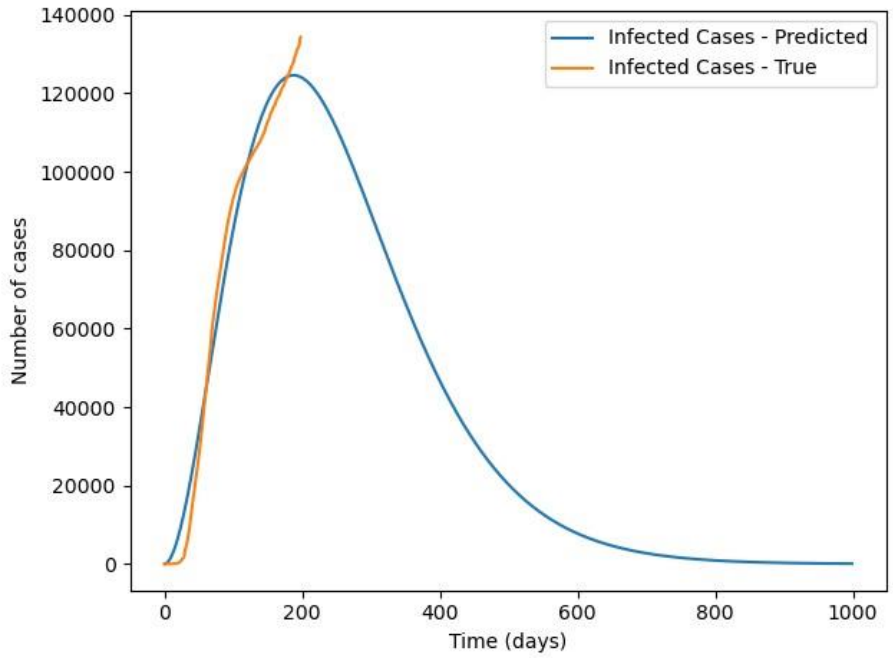

Fig.9. Infection Modelling using a Planck Function (α=3)

For equation (31, α=2), the optimal parameters are estimated to be 0.0023238 and 2.070922, respectively. For equation (31, α=3), the optimal parameters are estimated to be 0.0150317 and 0.297709, respectively. By observing the figures for both equations, it can be noticed that the extrapolated curves reflect similar properties as the infection curve, namely asymmetry.

4. Discussion

4.1. *SIR Model Interpretations*

The S-curve graph illustrates a gradual decline, indicating a slow rate of infection for the contagious disease. The I-curve graph shows a continuous increase in infected individuals meaning the susceptible population is still being infected. An inflection point in the curve would suggest the peak of infection has been reached which may not be visible using the variable, time (t), in the earlier stages of the spread. For this reason, it is important to be able to use the *s*, *i*, and *r* variables independently to derive the inflection point without depending on time (t) as a variable.

In this case, the condition to determine an inflection point are as follows:

$$\frac{ds}{dt} = -\beta si \tag{32a}$$

$$s" = \frac{d^2 s}{dt^2} \tag{32b}$$

For an inflection point to occur, *s*" = 0 and *si* are constant

$$\frac{ds}{dt} i + \frac{di}{dt} s = 0 \tag{32c}$$

$$\frac{di}{dt} = \beta si - \gamma i \tag{32d}$$

Equation (32c) can be rewritten as:

$$\frac{ds}{dt} i = -s \frac{di}{dt} = -si(\beta s - \gamma) \tag{32e}$$

Factoring out *i*, we have a simplification,

$$\frac{ds}{s} = -(\beta s - \gamma) dt \tag{32f}$$

or

$$\frac{ds}{s(\beta s - \gamma)} = -dt \rightarrow \int \left(\frac{1}{s} - \frac{\beta}{\beta s - \gamma}\right) ds = \gamma \int dt \tag{32g}$$

$$\log(s) - \log(\beta s - \gamma) = \gamma t \rightarrow \log\left(\frac{s}{\beta s - \gamma}\right) = \gamma t \tag{32h}$$

$$t_{inflection} = \frac{\log(s) - \log(\beta s - \gamma)}{\gamma} \tag{32i}$$

The R-curve graph also shows a continued increase, indicating an increase in number of recovered or deceased individuals. Given Canada's current situation, there appears to be far more individuals recovered than deceased; as such, it can be inferred that the R-curve is indicating good recovery [4].

4.2. *SEIR Model and Social Distancing*

Social distancing is the practice of reducing physical contact in order to reduce opportunity for the spread of transmissible diseases [7]. Common practices include social isolation, self-quarantine and cancellation of mass gatherings. Matrajt and Leung used a mathematical model to investigate effectiveness of social distancing in an average sized city [20]. The results suggested that implementing social distancing measures earlier in an epidemic will delay the epidemic curve while interventions implemented later will flatten the curve. The model also illustrated that the epidemic will rebound when interventions are suspended, indicating the importance of maintaining social distancing practices for the safety of the population [20].

To better understand the impact of social distancing practices, the following case study of United Kingdom (UK)'s and New Zealand's response to COVID-19 will serve as an example.

While many nations implemented physical distancing as a mandatory measure to slow down the spread of COVID-19, UK's government had deemed the virus as inevitable and pushed to suppress it, rather than eradicate it [41, 2]. The UK government initially implemented lax prevention methods to protect vulnerable groups such as the elderly and immunocompromised [41]. However, individuals did not take any measures to protect themselves and others until stricter lockdown measures were implemented, at which point COVID-19 cases had risen [36, 35]. After citizens took a more active stance in following protective measures, a small decline in daily case counts was observed [36]. Conversely, New Zealand is one of the only countries in the world to completely eradicate COVID-19 where strict measures were set early in the year [25, 27]. New Zealand's rapid response and social distancing methods allowed the country to completely open with no limits to public gatherings or public transportation. Schools and workplaces resumed without restrictions and mandatory requirements [26, 23, 10]. Both these cases demonstrated the necessity in rapid social distancing measures, and strict adherence of individual precautions, in order to control the spread of infection [36].

A more local case study can be seen in Canada's current COVID-19 situation. In recent work [38], the SEIRm model results displayed the following results. It was noticed that the mixing factor, *m*, decreased rapidly to 0.2 levels over approximately the first 150 days since April 10, 2020. The *m* factor then proceeds to increase to 0.3779

by September 16, 2020 [38].

The *m* factor in the SEIRm model plays a crucial part in the significance of this model. The values of the m factor indicate the severity of the situation regarding COVID-19 case numbers. As indicated earlier, the greater the value of *m*, the more severe the situation. Regarding COVID-19, if a greater *m* value was seen, this would indicate that numbers are rising which then puts greater pressure on hospitals due to rapid increase in patients. A higher *m* value would not only effect hospitals but would also impact equipment manufacturing companies and companies that are working to develop a vaccine for COVID-19. Alternatively, a lower *m* value would indicate a more controlled or lower number of COVID-19 cases. This lessens the strain on hospitals, personal protection equipment manufacturers, and labs working on vaccine development. Moreover, the *m* value also allows for a hypothetical timeline to be developed. A timeline would be a very useful aid in creating a plan for various areas in order to properly control the spread of COVID-19.

This study's results on the SEIR curve also analyzed the effect of social distancing on reducing cases. The ρ indicating level of social distancing - 0 to 1, everyone quarantined to no one quarantined respectively - showed the following trends. All curves remained relatively the same despite rho levels above 0. It is interesting to note however, in the E-Curve, the no social distancing group had the highest number of exposed cases at the fastest rate when compared to other social distancing levels. Overall, these results illustrate the importance social distancing as a method to mitigate the chance of exposure to the virus. Using these results, it's possible to create a plan of action, for not only any other biological outbreaks, but for the upcoming future as the world starts to make its way back into a sense of normalcy. The data involving social distancing allows institutions such as school boards, workplace unions and other councils of authority to create plans to protect individuals by interpreting the importance of social distancing and other protection methods. This will allow the best protection for citizens as they once again, enter back into the physical world.

4.3. *Planck Blackbody Distribution and Infectivity*

The simulations using the Planck function show the asymmetry of the data curves in a more realistic way than by using a symmetric function. The constants C_1 and C_2 were obtained by an accurate estimate using Least Squares Optimization to model the actual data. The predicted infection curve of equation (31, α=2) shows a longer period of steady increase compared to the predicted curve of equation (31, α=3). The later model estimated a sharp increase in number of cases during approximately the first 200 days. The number of cases then proceed to decrease at a slower rate over time. The first model (α=2) achieved an MSE of 121338312.79, while the second model (α=3) achieved a lower value of 35690796.88 – improving performance by 70.59%. Therefore, the second model (α=3) shows better fit to the actual data based on MSE metrics. By observing the figures for both equations, it can be noticed the extrapolated curves reflect similar properties as the infection curve – namely asymmetry.

5. Conclusions

The equations used in the SIR model were time dependent [8]. This study has examined not only the time-dependent equations but also derived the different variable relationships to one another. Specifically, this study derived the equation for number of infected cases depending on the number of susceptible individuals, which in turn was found with respect to removed individuals. These equations allow for study of infection in relation to transmission. That is, using these models, one can now mathematically study the relationship between infected, susceptible and removed individuals in epidemic models.

With the SEIR model, this study wanted to examine the impact of protective procedures on reducing disease spread. The equations were modelled to account for the effect of social distancing on the SEIR model - particularly, the exposed and infected groups by the variable ρ [40]. As seen in Figures 6 and 7, our results demonstrated the severe declining trends of case counts in infection and exposure when social distancing procedures were adhered to by everyone in a population. While the feasibility of complete adherence is difficult, these results support ideas of protective measures in reducing exposure - therefore, infection - of disease.

To our knowledge, no other study has examined COVID-19 transmission with respect to the SIR model using specific variable related derivations, the SEIR model with focus on impact of social distancing and the similarities of the infection curves to Planck blackbody functions. This study presented several mathematical approaches for the modelling of disease transmission using methodologies ranging from the SIR model to the SEIR model, and simulations by the Planck Blackbody function. Specifically, it demonstrated practical

applications of these models by comparing their results fitted onto the Canadian COVID-19 cases data. Through the predicted values from each model, meaningful inferences about the behaviour and trajectory of the COVID-19 pandemic were drawn.

Understanding COVID-19 transmission and examining potential ways to model this ever-evolving disease has become more important than ever. The return to businesses, schools and life prior to the pandemic, has been met with a rising trend of COVID-19 cases [4]. As mentioned, in the SEIRm model trials, the *m* factor had increased from 0.25 to 0.38. This indicates that at this higher value of *m*, there is a higher level of infectivity; so much so, that there are serious concerns of explosive growth of COVID-19 cases. To further add to concerns, if not curbed or lowered, this high infectivity will lead to a rise in COVID-19 cases in Canada which could overburden the health care system as early as late February 2021. That is, there will be an abundance of case growth before a vaccine can be developed, mass produced and widely administered in Canada [38]. Again, this stresses the importance of social distancing and lowering the *m* value to manageable levels.

As the COVID-19 situation continues to evolve and expand, the importance of examining COVID-19 transmission patterns becomes imperative. The results of this study can be used to better understand - or help confirm - the trends of COVID-19 transmission in a Canadian context. Further studies can use this data to further investigate the efficacy of using these mathematical models in extrapolating COVID-19 transmission trends.

6. **Acknowledgement**

The authors would like to thank Dr. Ken Roberts for his inspiring discussions that have resulted in an improved version of our manuscript. The authors would also like to thank Frank Li for his help in establishing some early coding and stimulating discussion.

References

[1] Grifoni A;Weiskopf D;Ramirez SI;Mateus J;Dan JM;Moderbacher CR;Rawlings SA;Sutherland A;Premkumar L;Jadi RS;Marrama D;de Silva AM;Frazier A;Carlin AF;Greenbaum JA;Peters B;Krammer F;Smith DM;Crotty S;Sette A; *Targets of T Cell Responses to SARS-CoV-2 Coronavirus in Humans with COVID-19 Disease and Unexposed Individuals*. url: https://pubmed. ncbi.nlm.nih.gov/32473127/.

[2] Martin Armstrong. *Infographic: The Best and Worst Rated National COVID19 Responses*. June 2020. url: https://www.statista.com/chart/ 21928/approval-ratings-national-covid-19-responses/.

[3] *Blackbody Radiation*. url: https://www.cv.nrao.edu/course/astr534/ BlackBodyRad.html.

[4] Public Health Agency of Canada. *Coronovirus Disease (COVID-19)*. Aug. 2020. url: https://www.canada.ca/en/public-health/services/ diseases/coronavirus-disease-covid-19.html.

[5] Jose M. Carcione et al. "A Simulation of a COVID-19 Epidemic Based on a Deterministic SEIR Model". In: *Frontiers in Public Health* 8 (2020). doi: 10.3389/fpubh.2020.00230. url: https://www.frontiersin. org/articles/10.3389/fpubh.2020.00230/full.

[6] David Celentano. *Gordis Epidemiology*. Elsevier, 2019.

[7] Yi-Cheng Chen et al. *A Time-dependent SIR model for COVID-19 with Undetectable Infected Persons*. 2020. arXiv: 2003.00122[q-bio.PE].

[8] *Classical deterministic contagious epidemic models without vital dynamics*. 2020. url: https://www.researchgate.net/publication/341250851_ epidemic_Classical_deterministic_contagious_epidemic_models_ without_vital_dynamics.

[9] R. M. Corless et al. "On the Lambert W function". In: *Advances in Computational Mathematics* 5.1 (1996), pp. 329–359. doi: 10.1007/bf02124750. url: https://link.springer.com/article/10.1007/BF02124750# citeas.

[10] *COVID-19 - current cases*. url: https://www.health.govt.nz/ourwork/diseases-and-conditions/covid-19-novel-coronavirus/ covid-19-current-situation/covid-19-current-cases.

[11] Paul Erdös and Alfred Rényi. "On the evolution of random graphs". In: *Publ. Math. Inst. Hungary. Acad. Sci.* 5 (1961), pp. 17–61.

[12] Alberto Godio, Francesca Pace, and Andrea Vergnano. "SEIR Modeling of the Italian Epidemic of SARS-CoV-2 Using Computational Swarm Intelligence". In: *International Journal of Environmental Research and Public Health* 17.10 (2020), p. 3535. doi: 10.3390/ijerph17103535. url: https://www.ncbi.nlm.nih.gov/pmc/articles/PMC7277829/.

[13] Robert Jeffrey and David Jeffrey. "The Lambert W Function". In: *The Princeton Companion to Applied Mathematics* (2015). doi: 10.1515/ 9781400874477. url: https://xueyuechuan.me/files/The%20Princeton% 20Companion%20to%20Applied%20Mathematics.pdf.

[14] Barbara Jester, Timothy Uyeki, and Daniel Jernigan. "Readiness for Responding to a Severe Pandemic 100 Years After 1918". In: *American Journal of Epidemiology* (2018). doi: 10.1093/aje/kwy165. url: https:// academic.oup.com/aje/article/187/12/2596/5068408?guestAccessKey= 2b05a8ed-3663-45c1-9fb2-96bff3b45f62.

[15] *Kermack-McKendrick Model*. url: https://mathworld.wolfram.com/ Kermack-McKendrickModel.html.

[16] W. O. Kermack and A. G. McKendrick. "A Contribution to the Mathematical Theory of Epidemics". In: *The Royal Society* 115.772 (Aug. 1927), pp. 700–721. doi: https://doi.org/10.1098/rspa.1927.0118.

[17] J Kranz. "Comparison of Epidemics". In: *Annual Review of Phytopathology* 12.1 (1974), pp. 355–374. doi: 10.1146/annurev.py.12.090174. 002035.

[18] H. G. Landau. “On some problems of random nets”. In: *The Bulletin of Mathematical Biophysics* 14.2 (1952), pp. 203–212. doi: 10.1007/ bf02477719. url: https://link.springer.com/article/10.1007/ BF02477719.

[19] Geng Li et al. “Coronavirus infections and immune responses”. In: *Journal of Medical Virology* 92.4 (Jan. 2020). doi: 10.1002/jmv.25685.

[20] Laura Matrajt and Tiffany Leung. “Evaluating the Effectiveness of Social Distancing Interventions to Delay or Flatten the Epidemic Curve of Coronavirus Disease”. In: *Emerging Infectious Diseases* 26.8 (2020), pp. 1740– 1748. doi: 10.3201/eid2608.201093. url: https://wwwnc.cdc.gov/ eid/article/26/8/20-1093_article.

[21] Christina E. Mills, James M. Robins, and Marc Lipsitch. “Transmissibility of 1918 pandemic influenza”. In: *Nature* 432.7019 (2004), pp. 904–906. doi: 10.1038/nature03063. url: https://www.nature.com/articles/ nature03063?page=21.

[22] Jeffrey Moehlis. *An SEIR Model*. 2002. url: https://sites.me.ucsb.edu/~moehlis/APC514/tutorials/tutorial_seasonal/node4.html.

[23] Beth Mole. *New Zealand has beaten COVID-19. Here’s how*. June 2020. url: https://arstechnica.com/science/2020/06/new-zealandeliminates-covid-19-lifts-all-social-distancing/.

[24] Carl R Nave. *Blackbody Radiation*. url: http://hyperphysics.phyastr.gsu.edu/hbase/mod6.html.

[25] *New Zealand beat Covid-19 by trusting leaders and following advice – study*. July 2020. url: https://www.theguardian.com/world/2020/ jul/24/new-zealand-beat-covid-19-by-trusting-leaders-andfollowing-advice-study.

[26] *New Zealand lifts all Covid restrictions, declaring the nation virus-free*. June 2020. url: https://www.bbc.com/news/world-asia-52961539.

[27] *New Zealand takes early and hard action to tackle COVID-19*. url: https: //www.who.int/westernpacific/news/feature-stories/detail/ new-zealand-takes-early-and-hard-action-to-tackle-covid-19.

[28] Michael Nikolaou. “Using Feedback on Symptomatic Infections to Contain the Coronavirus Epidemic: Insight from a SPIR Model”. In: (2020). doi: 10.1101/2020.04.14.20065698.

[29] *Notes on Solutions of SIR-Type Epidemic Models*. 2020.

[30] Manuel Rojas et al. “Convalescent plasma in Covid-19: Possible mechanisms of action”. In: *Autoimmunity Reviews* 19.7 (2020), p. 102554. doi: 10.1016/j.autrev.2020.102554. url: https://www.sciencedirect. com/science/article/pii/S1568997220301166.

[31] Hussin A. Rothan and Siddappa N. Byrareddy. “The epidemiology and pathogenesis of coronavirus disease (COVID-19) outbreak”. In: *Journal of Autoimmunity* 109 (2020), p. 102433. doi: 10.1016/j.jaut.2020. 102433.

[32] *SIR Model*. url: https://mathworld.wolfram.com/SIRModel.html.

[33] David Smith and Lang Moore. *The SIR Model for Spread of Disease, The Differential Equation Model*. Dec. 2004. url: https://www.maa. org/press/periodicals/loci/joma/the-sir-model-for-spread-ofdisease-the-differential-equation-model.

[34] Ray Solomonoff and Anatol Rapoport. “Connectivity of random nets”. In: *The Bulletin of Mathematical Biophysics* 13.2 (1951), pp. 107–117. doi: 10.1007/bf02478357. url: http://raysolomonoff.com/publications/ 50.pdf.

[35] Conor Stewart. *Measures to protect against COVID-19 in Great Britain 2020*. July 2020. url: https://www.statista.com/statistics/1101634/ measures-to-protect-against-covid-19-in-great-britain/.

[36] Conor Stewart. *UK: COVID-19 new cases by day*. July 2020. url: https:

//www.statista.com/statistics/1101947/coronavirus-casesdevelopment-uk/.

[37] Jeffery K. Taubenberger and David M. Morens. “1918 Influenza: the Mother of All Pandemics”. In: *Emerging Infectious Diseases* 12.1 (2006), pp. 15– 22. doi: 10.3201/eid1209.05-0979. url: https://wwwnc.cdc.gov/ eid/article/12/1/05-0979_article.

[38] *Unpublished raw data of Dr. Ken Roberts regarding SEIRm simulations of Canadian COVID-19 cases*. 2020.

[39] S R Valluri, D J Jeffrey, and R M Corless. “Some applications of the Lambert W function to physics”. In: *Canadian Journal of Physics* 78.9 (2000), pp. 823–831. doi: 10.1139/p00-065. url: https://ir.lib.uwo.ca/cgi/viewcontent.cgi?article=1028&context=physicspub.

[40] Peter J. Witbooi, Grant E. Muller, and Garth J. Van Schalkwyk. “Vaccination Control in a Stochastic SVIR Epidemic Model”. In: *Computational and Mathematical Methods in Medicine* 2015 (2015), pp. 1–9. doi: 10.1155/2015/271654. url: https://www.hindawi.com/journals/comm/2015/271654/.

[41] Ed Yong. *The U.K.’s Coronavirus ’Herd Immunity’ Debacle*. Mar. 2020. url: https://www.theatlantic.com/health/archive/2020/03/ coronavirus-pandemic-herd-immunity-uk-boris-johnson/608065/.